Ultrasonics Sonochemistry 111 (2024) 107089

Contents lists available at ScienceDirect

Ultrasonics Sonochemistry

journal homepage: www.elsevier.com/locate/ultson

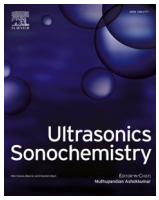

Enhancement of extraction efficiency and functional properties of chickpea protein isolate using pulsed electric field combined with ultrasound treatment

Xin-Jue Lai [a,1], Jian-Quan Chen [a,1], Jing Nie [a], Pei-Feng Guo [a], Muhammad Faisal Manzoor [a], Yan-Yan Huang [a], Jian Li [a,b], Song-Yi Lin [c], Xin-An Zeng [a,b], Rui Wang [a,*]

[a] School of Food Science and Engineering, Guangdong Provincial Key Laboratory of Intelligent Food Manufacturing, Foshan University, Foshan 528225, China
[b] School of Food Science and Engineering, South China University of Technology, Guangzhou 510641, China
[c] National Engineering Research Center of Seafood, School of Food Science and Technology, Dalian Polytechnic University, Dalian 116034, China

ARTICLE INFO

Keywords:
Pulsed electric field
Ultrasound
Chickpea protein isolate
Optimisation
Functional properties

ABSTRACT

Chickpea protein isolate (CPI) is a promising dietary protein with the advantages of low allergenicity, easy digestion and balanced composition of essential amino acids. However, due to the thick skin of chickpeas, the extraction of CPI is challenging, resulting in lower efficiency of the alkaline extraction-isoelectric precipitation (AE-IEP) method. Therefore, the present study investigated the effect of pulsed electric field combined with ultrasound (PEF-US) treatment on the extraction efficiency of CPI and the functional properties was characterized. Parameter optimization was carried out using response surface methodology (RSM), with the following optimized conditions: pulse duration of 87 s, electric field intensity of 0.9 kV/cm, ultrasonic time of 15 min, and ultrasonic power of 325 W. Under the optimized conditions, the yield of CPI after combined (PEF-US) treatment was 13.52 ± 0.13 %, which was a 47.28 % improvement over the AE-IEP method. This yield was better than that obtained with either individual PEF or US treatment. Additionally, the functional properties (solubility, emulsification, and foaming) of CPI were significantly enhanced compared to AE-IEP. However, the stability of emulsification and foaming did not show significant differences among the four methods. The PEF-US method efficiently extracts CPI with excellent functional properties, enabling the production of proteins as desired functional additives in the food industry.

1. Introduction

Proteins play a key role in determining the nutrition, texture and structure of numerous food products. Despite their superior functional and sensory properties, animal proteins are more expensive to produce than plant proteins, have a greater environmental impact, and may increase the risk of cardiovascular disease when consumed over time [1]. Alternative proteins are gaining popularity due to concerns about low carbon and health. Cereals, pulses, nuts, fungi (mushrooms) and algae all provide alternative proteins for use in food products [2–6]. Chickpea protein isolate (CPI) is notably a rich source of lysine, a nutrient lacking in cereal proteins. Incorporating CPI powder into cereal products can enhance protein utilization, nutritional content, and sensory properties [7]. CPI has good functional properties, such as solubility, emulsification, and foaming, but these excellent properties mostly depend on the protein extraction method [8]. As a result, CPI has considerable potential for further research and application in the food business.

The selection of an effective CPI extraction method is crucial for improving protein yield and purity, which is conducive to promoting the efficient use of CPI in industrial applications. The primary method for extracting CPI involves alkaline extraction-isoelectric precipitation (AE-IEP) treatment [9]. While this technique is relatively simple and inexpensive, it often results in low protein yield and purity, as well as high intracellular protein residues [10]. Moreover, under extreme alkaline or prolonged extraction conditions, the electrostatic repulsion between protein molecules increases, leading to protein denaturation [11]. Additionally, the robust nature of chickpea cell walls, as evidenced by

* Corresponding author.
E-mail address: ruiwang@fosu.edu.cn (R. Wang).
[1] These authors contributed equally to this work.

https://doi.org/10.1016/j.ultsonch.2024.107089
Received 8 August 2024; Received in revised form 24 September 2024; Accepted 27 September 2024
Available online 28 September 2024

the observed structural integrity following in vitro digestion compared to other legumes, presents challenges in protein extraction efficiency [12]. Therefore, it is imperative to explore alternative, cost-effective approaches to enhance CPI extraction rates and yields.

The use of physical methods such as high-pressure homogenisation (HPH) and microwave (MW) treatment can effectively break down the tough cell walls of chickpeas, leading to increased protein solubility and extraction rate. However, HPH may not only break down cell walls but also damage protein structure, reducing protein solubility [13]. Similarly, the MW treatment can denature proteins due to thermal effects [14]. Pulsed electric field (PEF) technology appears to be an effective plant protein extraction technique. PEF is a non-thermal technology that provides efficient, gentle, and targeted protein extraction. The electric field generates pores in cell membranes and walls, facilitating the release and solubilisation of proteins [15]. Kronbauer et al. [16] demonstrated successful extraction of nettle leaves proteins using PEF, and the yield of soluble proteins obtained from 5 min treatment was more than 60 % within the optimised interval of PEF treatment (specific energy between 10 and 24 kJ kg^{-1}, and 70–80 ℃). However, we used PEF to extract the CPI and found that the improvement in the CPI extraction rate was limited, with only a 22.13 % improvement in AE-IEP. In addition, excessive pulse duration and field intensity during PEF treatment were found to reduce protein yield. Thus, it is imperative to investigate the combined application of diverse technological approaches to optimize protein extraction efficiency.

Pulsed electric field combined with ultrasound (PEF-US) is an emerging multi-physical field coupling processing technology that has gained attention in recent years. Studies have shown that PEF-US can effectively extract polyphenolic substances from litchi peel, resulting in a total phenol content 2.3 times higher than traditional hot water extraction methods [17]. Similarly, in the extraction of total flavonoids from *Pericarpium Citri Reticulatae* (PCR), PEF-US was found to be more efficient compared to other extraction methods such as hot water extraction (HAE), US extraction, PEF extraction and macroporous resin [18]. The PEF treatment effectively breaks through cell walls to promote the release of proteins, while the cavitation effect of US leads to the formation and collapse of small bubbles in the liquid, generating shock waves that enhance the interaction between proteins and external solutes. Then, considering the characteristics of the two mentioned above, it is worthwhile to investigate in-depth whether the combination of PEF and US will have synergistic effects and thus improve the rate of CPI acquisition.

Therefore, the aim of this study was to investigate the feasibility of PEF-US treatment in improving CPI extraction and to determine the optimal extraction conditions using response surface methodology (RSM). It was also noted that PEF and US may have modifying effects on the structure and functional properties of CPI. Therefore, the study characterized the structure (circular dichroism and fluorescence) and functional properties (solubility, emulsification, and foaming) of proteins treated with the PEF-US method. The findings of this research aim to offer novel methods and insights for the efficient extraction and effective modification of CPI.

2. Materials and methods

2.1. Materials

Chickpeas seeds were purchased from Xinjiang Tianshan Qidou Biotechnology Co. 5,5′-Dithionitrobenzoic acid (DTNB) was obtained from Shanghai McLean Biochemical Technology Co. 8-Anilino-1-naphthalenesulfonic acid (ANS), bicinchoninic acid assay (BCA) protein kit, were obtained from Shanghai Yuanye Biotechnology Co. The chemical reagents used in this research were all analytical grades without further purification.

2.2. Chickpea preparation

Chickpea flour was prepared by referring to the method of Byanju et al. [19]. The chickpea flour was defatted using petroleum ether at a mass-volume ratio of 1:2. The mixture was stirred for 60 min at room temperature, then centrifuged. This process was repeated twice, and the resulting precipitate was air-dried to obtain defatted chickpea flour, which was stored at 4 ℃.

2.3. Alkaline extraction-isoelectric precipitation (AE-IEP)

CPI was extracted by AE-IEP with suitable modifications [20]. The isoelectric point of CPI was determined to be 4.0 using a Microplate reader (DLJ-100, Nanjing Di Lejia Biotechnology Co., China) according to the previous reported method (Fig. S1) [21]. In brief, chickpea flour was mixed with ultrapure water in a mass-volume ratio of 1:10, the pH was adjusted to 9 with 1 M NaOH, and stirred for 1 h at room temperature. The resulting solution was centrifuged at 8000 r/min for 10 min, and the supernatant was collected. The supernatant was adjusted to the isoelectric point 4.0 with 1 M HCl and left at 4 ℃ for 20 min to settle the protein, centrifuged under the same conditions as described above, the precipitate was washed twice, centrifuged again, and the protein was resolubilised and adjusted to a neutral pH of 7.0 and then spread uniformly in a plastic dish for lyophilisation to obtain CPI. The formula for calculating protein yield was as follows:

$$\text{yield}\,(\%) = \frac{\text{Weight of protein obtained by lyophilisation}\,(g) \times \text{Protein purity}}{\text{Weight of raw materials}\,(g)} \times 100\% \quad (1)$$

Where protein purity (85.2 %) was measured by the Kjeldahl method. (AOAC International) [22].

2.4. Extraction of CPI by PEF, US and PEF-US treatment

The process of extracting chickpea protein by PEF, US and PEF-US treatment in this study was summarized in Fig. 1. Chickpea flour was mixed with water in a mass to volume ratio of 1:10. Protein extraction was carried out using PEF equipment (EX-1900, Guangzhou Pahu Technology Co., China) after alkaline extraction for 1 h. The solution was then transferred to the PEF treatment chamber, where the pulse width was set at 5 μs and the pulse frequency at 100 Hz. The temperature was maintained at 20–25 ℃ during the treatment process by using a water circulation system with the temperature set at 4 ℃. The pulse durations were set to 30, 60, 90, 120, and 150 s, with pulse field intensity of 0.7, 0.8, 0.9, 1.0, and 1.1 kV/cm. The intensity of the electric field was calculated by dividing the actual voltage displayed on the oscilloscope by the height of the sample. The solution after PEF treatment underwent centrifugation at 8000 r/min for 10 min to collect the supernatant, which then underwent further processing as detailed in Section 2.3 to obtain CPI.

US treatment involved sonication of the solution after 1 h of stirring,

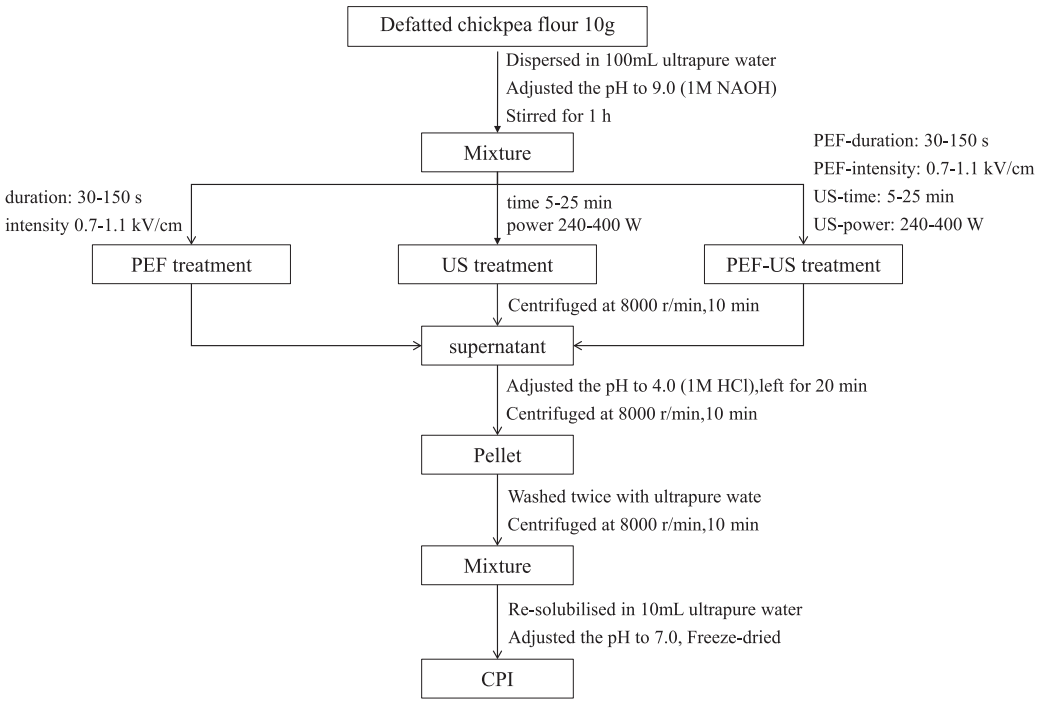

Fig. 1. Protein extraction protocol from defatted chickpea flour utilizing PEF, US, and PEF-US treatment based on the AE-IEP method.

with the probe fully extended into the solution within the sonication cup (LJ-JY92-ZZN, Shanghai Li-Chen Bang Xi Instrument Technology Co., China). The temperature was maintained at 20–25 ℃ during the treatment process by using an ice bath. Sonication was carried out in intervals (0.8 s on and 2 s off) with time (5, 10, 15, 20 and 25 min) and power (240, 280, 320, 360 and 400 W). The treated solution was centrifuged, the supernatant collected, and acid added for precipitation (as described in Section 2.3) to obtain CPI.

In the combined PEF and US treatment, the solution underwent PEF treatment first, followed by transfer to a sonication cup for US treatment under the same parameters. The resulting extracts were collected as PEF-US samples for further analysis.

2.5. Responsive surface design

Based on the results of the single-factor experiment, a four-factor, three-level Box-Behnken (BBD) experiments was designed, with pulse duration (X_1: 60, 90, and 120 s), pulse field intensity (X_2: 0.8, 0.9, and 1.0 kV/cm), ultrasonic time (X_3: 10, 15, and 20 min), and ultrasonic power (X_4: 280, 320, and 360 W) selected as the test factors, and protein yield (Y) as the response value. A total of 29 groups were included in this experiment and all the tests were conducted in triplicate and analyzed using Design-Expert Software 12.0.1 (Stat-Ease Inc., Minneapolis, USA) to obtain a second-order polynomial equation as follows:

$$Y = \beta 0 + \sum_{i=1}^{4} \beta_i X_i + \sum_{i=1}^{4} \beta_{ii} X_i^2 + \sum_{i<j=2}^{4} \beta_{ij} X_i X_j \quad (2)$$

Where Y is the response value, β_0, β_i, β_{ii} and β_{ij} denote the regression coefficients of the intercept, linear, quadratic and interaction terms, respectively. The above equation describes the relationship between the response values and the terms in the model, and is an algebraic representation of the response surface that is able to demonstrate that the relationship between the response values and the factors is nonlinear. X_i, X_j denote the independent variables, and X_iX_j denote the interaction terms between the factors.

2.6. Scanning electron microscope (SEM)

The surface morphology of CPI was analyzed using a SEM (ZEISS Sigma 500, Carl Zeiss AG, Germany). The samples were coated with gold and examined under high vacuum conditions at an accelerating voltage of 5.00 kV, with magnifications of 250.

2.7. Circular dichroism (CD)

The CD spectra were determined using the method proposed by Xiong et al., with appropriate adjustments as needed [23]. The CPI was dissolved in 10 mM phosphate buffer at pH 7.0 and centrifuged at 10,000 g for 15 min. 200 μL of 0.25 mg/mL CPI solution was performed by using an automated CD chromatograph in the range from 200 to 260 nm (Chirascan TM V100, Applied Photo physics Ltd, Leatherhead, Britain). The secondary structure content of the CPI was calculated by the CDNN2.1 software (Applied Pho-tophysics, Ltd., Leatherhead, United Kingdom).

2.8. Intrinsic fluorescence

The CPI was dissolved in 10 mM phosphate buffer solution at pH 7.0 and diluted to 0.5 mg/mL. 3 mL of CPI solution was analyzed by using a Fluorescence spectrometer (F-4600, Hitachi, Ltd., Japanese). The CPI solution was placed in a 1 cm quartz cuvette. The excitation wavelength was 280 nm, and the emission spectra ranged from 290 to 500 nm. The excitation and emission slit widths were 5 nm, the scanning speed of 1200 nm/min, and the phosphate buffer solution was used as the blank.

2.9. Protein surface hydrophobicity (PSH)

The surface hydrophobicity of CPI was determined by the method of Wang et al., with slight modification [24]. CPI was dissolved in 10 mM phosphate buffer (pH 7.0) to formulate different concentrations (0.1, 0.3, 0.5, 0.7, 0.9, 1.0 mg/mL) of protein solutions. 20 μL of 8.0 mM ANS was mixed with 4 mL of protein solution and placed in the dark for 30 min. The excitation and emission wavelengths were set at 390 nm and 470 nm, respectively. The fluorescence intensity was plotted as the

vertical coordinate and the protein concentration as the horizontal coordinate. The slope of the starting segment of the obtained curve represented the value of PSH.

2.10. Protein solubility

The protein solution was collected using the method proposed by Patil et al., with slight modification [25]. Natural and modified CPI were mixed with distilled water and stirred for 2 h to obtain sample solution (10 mg/mL). The solution centrifuged at 10,000*g* for 10 min, the supernatant was taken and diluted 5-fold for absorbance measurement. The protein content of sample solution was determined by the BCA method. A standard curve ($y = 1.1616x + 0.1799$, $R^2 > 0.998$) was established by using bovine serum albumin (BSA). Solubility was presented as the ratio of the protein content in the supernatant to the protein content in the original sample.

2.11. Emulsifying properties

Determination of emulsion activity index (EAI) and emulsion stability index (ESI) for CPI based on the method of Tan et al. [26]. The CPI prepared after treatment under different conditions was dissolved in distilled water (10 mg/mL) and stirred for 2 h at 25 ℃. Subsequently, to prepare the emulsion, 12 mL of CPI solution was mixed with 3 ml of soybean oil and homogenized at 10000 g per min for 2 min to form a stable emulsion system. Next, 30 μ L of prepared emulsion was quickly mixed with 3 mL of 0.1 % SDS solution and the absorbance value was measured at 500 nm by a spectrophotometer. The emulsion was allowed to stand for 10 min and then the absorbance values were determined. The EAI and ESI were obtained from the following equations.

$$\mathrm{EAI}\,(m^2/g) = \frac{2 \times 2.303 \times A_0 \times D}{c \times (1 - \varnothing) \times 10000} \tag{3}$$

$$\mathrm{ESI}\,(\mathrm{min}) = \frac{A_{10}}{A_0} \times 100 \tag{4}$$

where c is the protein concentration (0.01 g/mL), D is the dilution factor (100), and ∅ is the oil phase volume fraction (20 %).

2.12. Foaming properties

The CPI prepared after treatment under different conditions was dissolved in distilled water (10 mg/mL) and stirred for 2 h at 25 ℃. 8 mL of the protein solution was taken and homogenized at 19000 rpm for 2 min. The volume of the foam was recorded at 2 min (V_2) and 30 min (V_{30}) respectively. Foaminess (FA) and foam stability (FS) are calculated according to the following equations.

$$\mathrm{FA}\,(\%) = \frac{V_2}{V_S} \tag{5}$$

$$\mathrm{FS}\,(\%) = \frac{V_{30}}{V_2} \tag{6}$$

where V_S is the initial liquid volume.

2.13. Statistical analysis

All analyses were performed in triplicate and all data were analyzed

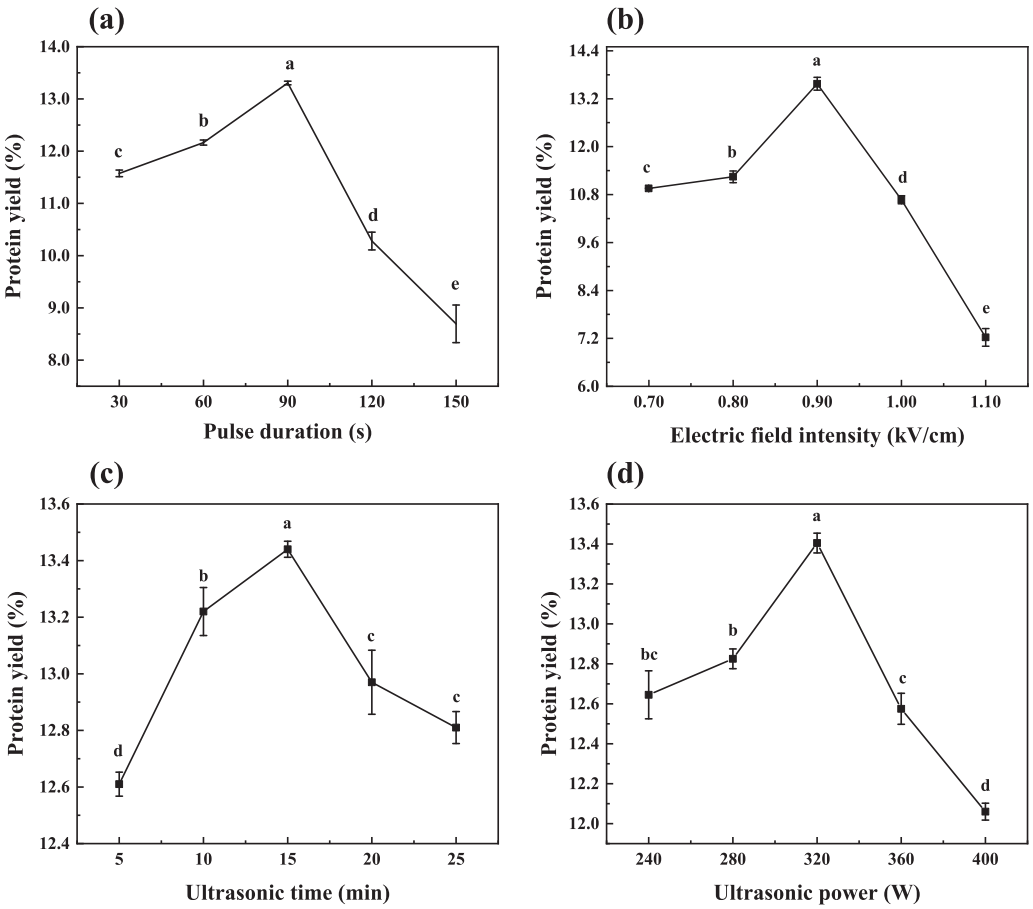

Fig. 2. Effect of PEF-US treatment on CPI yield. (a) pulse duration (s), (b) pulse field intensity (kV/cm), (c) ultrasonic time (min), (d) ultrasonic power (W). Results are presented as mean ± SD (n = 3). Different lowercase letters above the bars indicate significant differences determined by SPSS test ($p < 0.05$).

using analysis of variance (ANOVA) as well as Tukey's test for significant differences, significant p-values less than the set level of significance (0.05) were determined to be significant, and all data are presented as mean ± SD deviation.

3. Results and discussion

3.1. Single-factor results for extraction of CPI by PEF, US and PEF-US treatment

By single-factor optimization of PEF and US treatment, the optimal conditions for PEF treatment were obtained as a pulse duration of 90 s and electric field intensity of 0.9 kV/cm (Fig. S2). For US extraction, the optimum conditions were a treatment time of 15 min and ultrasonic power of 320 W. From the previous experiments, it was comprehended that both PEF and US treatment were facilitative to CPI yield. Consequently, we employed the combined (PEF-US) treatment for extracting CPI and investigated the optimal extraction conditions (Fig. 2). The impact of pulse duration and electric field intensity on CPI yield in PEF-US treatment was analyzed in Fig. 2a and b. As pulse duration and electric field intensity increased, yield initially rose before declining. The highest protein yield, at 13.33 ± 0.04 % and 13.46 ± 0.16 %, was observed at a pulse duration of 90 s and an electric field intensity of 0.9 kV/cm. Fig. 2c and d examined the influence of ultrasonic time and power on CPI yield, revealing that the highest yield occurred at 15 min of ultrasonic time and 320 W of ultrasonic power. In the Box-Behnken design, the design point should be a combination of high and low factor levels along with their midpoints. Therefore, pulse duration (60, 90, and 120 s), electric field intensity (0.8, 0.9, and 1.0 kV/cm), ultrasonic time (10, 15, and 20 min), and ultrasonic power (280, 320, and 360 W) were selected as the test factors for the response surface.

Table 1
Response surface BBD experimental design, CPI yield and predicted value.

Run	Independent Variables				Protein yield (%)	
	X_1[a]	X_2[b]	X_3[c]	X_4[d]	Expt.	Pred.
1	60 (−1)	0.9 (0)	10 (−1)	320 (0)	12.18	11.86
2	90 (0)	0.8 (−1)	15 (0)	360 (+1)	12.19	11.81
3	90 (0)	1.0 (+1)	15 (0)	280 (−1)	9.47	9.83
4	90 (0)	0.8 (−1)	15 (0)	280 (−1)	11.37	11.05
5	60 (−1)	0.8 (−1)	15 (0)	320 (0)	10.82	11.24
6	60 (−1)	0.9 (0)	20 (+1)	320 (0)	12.13	11.94
7	90 (0)	0.9 (0)	15 (0)	320 (0)	12.79	13.21
8	60 (−1)	0.9 (0)	15 (0)	280 (−1)	11.09	11.28
9	90 (0)	1.0 (+1)	10 (−1)	320 (0)	10.25	10.24
10	60 (−1)	0.9 (0)	15 (0)	360 (+1)	11.47	11.54
11	90 (0)	0.9 (0)	15 (0)	320 (0)	13.27	13.21
12	90 (0)	1.0 (+1)	15 (0)	360 (+1)	9.39	9.70
13	90 (0)	1.0 (+1)	20 (+1)	320 (0)	10.16	10.27
14	120 (+1)	0.9 (0)	20 (+1)	320 (0)	10.87	11.18
15	90 (0)	0.9 (0)	10 (−1)	280 (−1)	10.89	10.84
16	90 (0)	0.9 (0)	15 (0)	320 (0)	13.38	13.21
17	90 (0)	0.8 (−1)	20 (+1)	320 (0)	11.72	11.93
18	90 (0)	0.9 (0)	15 (0)	320 (0)	13.11	13.21
19	90 (0)	0.9 (0)	15 (0)	320 (0)	13.48	13.21
20	120 (+1)	0.8 (−1)	15 (0)	320 (0)	11.59	11.57
21	120 (+1)	0.9 (0)	15 (0)	360 (+1)	10.88	10.89
22	90 (0)	0.8 (−1)	10 (−1)	320 (0)	11.83	11.92
23	120 (+1)	0.9 (0)	10 (−1)	320 (0)	11.02	11.2
24	90 (0)	0.9 (0)	20 (+1)	280 (−1)	12.29	11.99
25	60 (−1)	1.0 (+1)	15 (0)	320 (0)	10.78	10.62
26	120 (+1)	0.9 (0)	15 (0)	280 (−1)	10.38	10.51
27	90 (0)	0.9 (0)	10 (−1)	360 (+1)	12.16	12.28
28	90 (0)	0.9 (0)	20 (+1)	360 (+1)	11.31	11.18
29	120 (+1)	1.0 (+1)	15 (0)	320 (0)	9.46	8.86

[a] X_1:pulse duration.
[b] X_2:electric field intensity.
[c] X_3:ultrasonic time.
[d] X_4:ultrasonic power.

Table 2
ANOVA of the responses and model fit statistics for regression models.

Source	Sum of squares	DF	Mean square	*F*-value	*p*-value
Model	35.39	14	2.53	19.28	<0.0001
X_1	1.52	1	1.52	11.59	0.0043
X_2	8.35	1	8.35	63.69	<0.0001
X_3	0.0019	1	0.0019	0.0143	0.9065
X_4	0.304	1	0.304	2.32	0.1501
X_1X_2	1.09	1	1.09	8.33	0.012
X_1X_3	0.0025	1	0.0025	0.0191	0.8921
X_1X_4	0.0036	1	0.0036	0.0275	0.8708
X_2X_3	0.0001	1	0.0001	0.0008	0.9784
X_2X_4	0.2025	1	0.2025	1.54	0.2343
X_3X_4	1.27	1	1.27	9.65	0.0077
X_12	7.71	1	7.71	58.79	<0.0001
X_22	15.49	1	15.49	118.12	<0.0001
X_32	2.13	1	2.13	16.22	0.0012
X_42	7.32	1	7.32	55.87	<0.0001
Residual	1.84	14	0.1311		
Lack of fit	1.54	10	0.1544	2.12	0.2447
Pure error	0.2917	4	0.0729		
Cor Total	37.23	28			
R^2	0.9507				
Adj R^2	0.9014				
Pred R^2	0.7489				
CV%	3.17				

X_1, X_2, X_3 and X_4 represent the same as above.

3.2. Statistical analysis and model fitting

Design-Expert 12.0.1 was used to design a four-factor, three-level BBD test, and the experimental results and predicted values were shown in Table 1. The experimental design consisted of 24 factorial points as well as 5 centroids and CPI yield were selected as the response value (Table 1). ANOVA was used to estimate the significance of factors and their interactions on the response values (Table 2). The response surface model was significant ($p < 0.01$) and the misfit term was not significant ($p = 0.2447 > 0.05$). It shows that the regression equation is highly credible and the unknown factors have less influence on the experimental results, thus the model can be used to predict the correlation of factors with CPI yield (Y). The *F*-value can be used to determine the extent to which the indicator is associated with the response. The factor that had the greatest effect on protein yield was electric field intensity (X_2), followed by pulse duration (X_1), ultrasonic power (X_4) and ultrasonic time (X_3). Among the interaction terms, the largest *F*-value was found for X_3X_4 interaction, followed by X_1X_2 interaction, indicating that the interaction between ultrasonic time and ultrasonic power was highly significant ($p < 0.01$), the interaction between pulse duration and electric field intensity was significant ($p < 0.05$) and the rest of the factor interactions were not significant. The relationship between each factor and protein yield (Y) can be expressed as a function:

$$Y = 13.21 - 0.3558X_1 - 0.8342X_2 + 0.0125X_3 + 0.1592X_4 - 0.5225X_1X_2 - 0.0250X_1X_3 + 0.0300X_1X_4 + 0.0050X_2X_3 - 0.2250X_2X_4 - 0.5625X_3X_4 - 1.09X_1^2 - 1.55X_2^2 - 0.5746X_3^2 - 1.06X_4^2$$

The regression coefficient R^2 of the equation reflects the ability of the regression equation to explain the response value (Y). The R^2 was 0.9507, which implied that the regression equation established in this study explained about 95 % of the variations in the response value. The closer the R^2 is to 1, the better the model is fitted. However, the different number of samples also affects the R^2. The adjusted regression coefficient (adj R^2) is able to cancel out the influence of sample size and thus assess the adequacy of the model more accurately. The adj R^2 (0.9014) indicated that 9.86 % of the total variation could not be explained by the model. Usually, adj R^2 between 0.8 and 1 represents a high degree of correlation between variables. The predicted regression coefficient (pred R^2) was 0.7489, while the coefficient of variation (CV) was 3.17 %, suggesting a real and reliable experimental result. The value between adj R^2 and pred R^2 are less than 0.2, indicating that the model can explain the process better. The CV demonstrates the precision of an

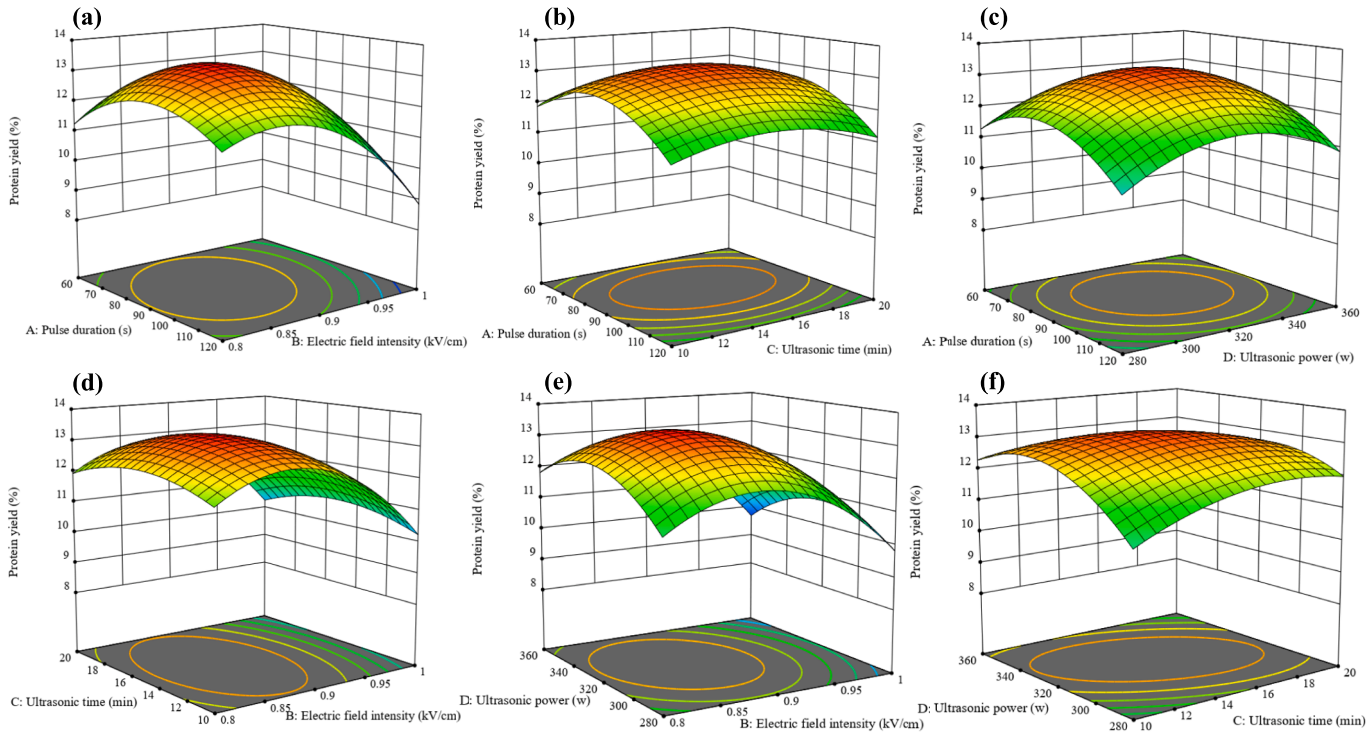

Fig. 3. Response surface 3D plot of the effect of interaction of factors on protein yield. (a) pulse time and pulsed field intensity interaction, (b) pulse time and ultrasonic time interaction, (c) pulse time and ultrasonic power interaction, (d) ultrasonic time and pulsed field intensity interaction, (e) ultrasonic power and pulsed field intensity interaction, (f) ultrasonic power and ultrasonic time interaction.

experiment, and the CV of less than 10 % signifies that the data are more stable and reproducible.

3.3. Effect of various factors on protein yield

The link between variables and response values (Y) was shown in three-dimensional (3-D) response surface plots (Fig. 3). The steeper the surface, the more strongly the variables affect the reaction value [27]. By keeping two factors constant, the interaction between them on CPI yield (Y) can be visualized. Protein yield increased with longer pulse durations (Fig. 3a, b & c). This might be attributed to the extended pulse treatment, which allowed for greater irreversible membrane perforation or prolonged recovery from reversible perforation, thereby enhancing the release of proteins from the cell in the experiment [28]. It can be seen from Fig. 3a, d & e that protein yield increased significantly when the electric field intensity increased from 0.8 to 0.9 ($p < 0.01$, Table 2). As the electric field intensity increased, the solvent penetrated into the cell faster, making it easier for the protein to permeate out. Fig. 3b, d & f illustrated that a longer ultrasonic time benefited the yield of Y. This was explained by the fact that the homogenization of the sample and solvent mixture through US treatment, leading to enhanced contact time and area between the solvent and material [29]. Y with increased ultrasound power from 280 W to 320 W (Fig. 3c, e & f). At lower ultrasonic power levels, the cavitation effect was not as pronounced, resulting in a lower protein yield. Vardanega et al. [30] proposed that ultrasonic treatment also induces hydration, causing the pores in the cell wall to expand. This facilitated a faster exchange of solvent within and outside the cell, ultimately leading to an increase in protein yield.

3.4. Validation tests of the model

According to the results of response surface optimisation and combined with the actual situation, the optimal process parameters for CPI were: pulse duration 87 s, electric field intensity 0.9 kV/cm, ultrasonic time 15 min, ultrasonic power 325 W. The predicted value of protein yield under this parameter was 13.341 %. Using the above conditions for three experimental validations, the protein yield was found to be 13.52 ± 0.13 %. Upon comparison, the relative error between the predicted and observed values was determined to be 1.32 %, indicating an error margin of less than 3 %. This confirmed the high accuracy of the model, verifying its validity. Consequently, the model is deemed applicable for theoretically interpreting the results of this experiment and holds guiding significance for practical operations.

3.5. Comparison of protein yield between AE-IEP, PEF, US and PEF-US treatment

The protein yield of chickpea resulting from four different treatments (AE-IEP, PEF, US, and PEF-US) were illustrated in Fig. 4b. The highest protein yield of 13.52 ± 0.13 % was obtained by PEF-US treatment. AE-IEP treatment gave a CPI yield of 9.18 ± 0.25 %. The protein yield of PEF-US was significantly ($p < 0.05$) increased by 47.28 % compared to AE-IEP treatment. In addition, PEF-US treatment also exhibited higher yield compared to the PEF (22.13 %) and US (20.07 %) treatment. The diagram of combining PEF and US to enhance the CPI extraction rate was illustrated in Fig. 5. To begin, PEF treatment of CPI, which results in a transmembrane potential difference greater than a threshold value, forms controlled micropores in the cell membrane and cell wall, allowing tiny molecules (protein) to enter and exit the cell [31]. Immediately following this, US treatment leads to a series of rapid compressions and expansions, creating shock breaks that increase the diffusion rate of protein molecules, allowing them to be released from the cell interior [32]. Fig. 4a showed the experimental pictures of isoelectric point precipitation of PEF-US and AE-IEP treatment, it was clearly observed that protein precipitation increased after PEF-US treatment. The results indicated that PEF-US treatment was a superior method for extraction of CPI as compared to single extraction method.

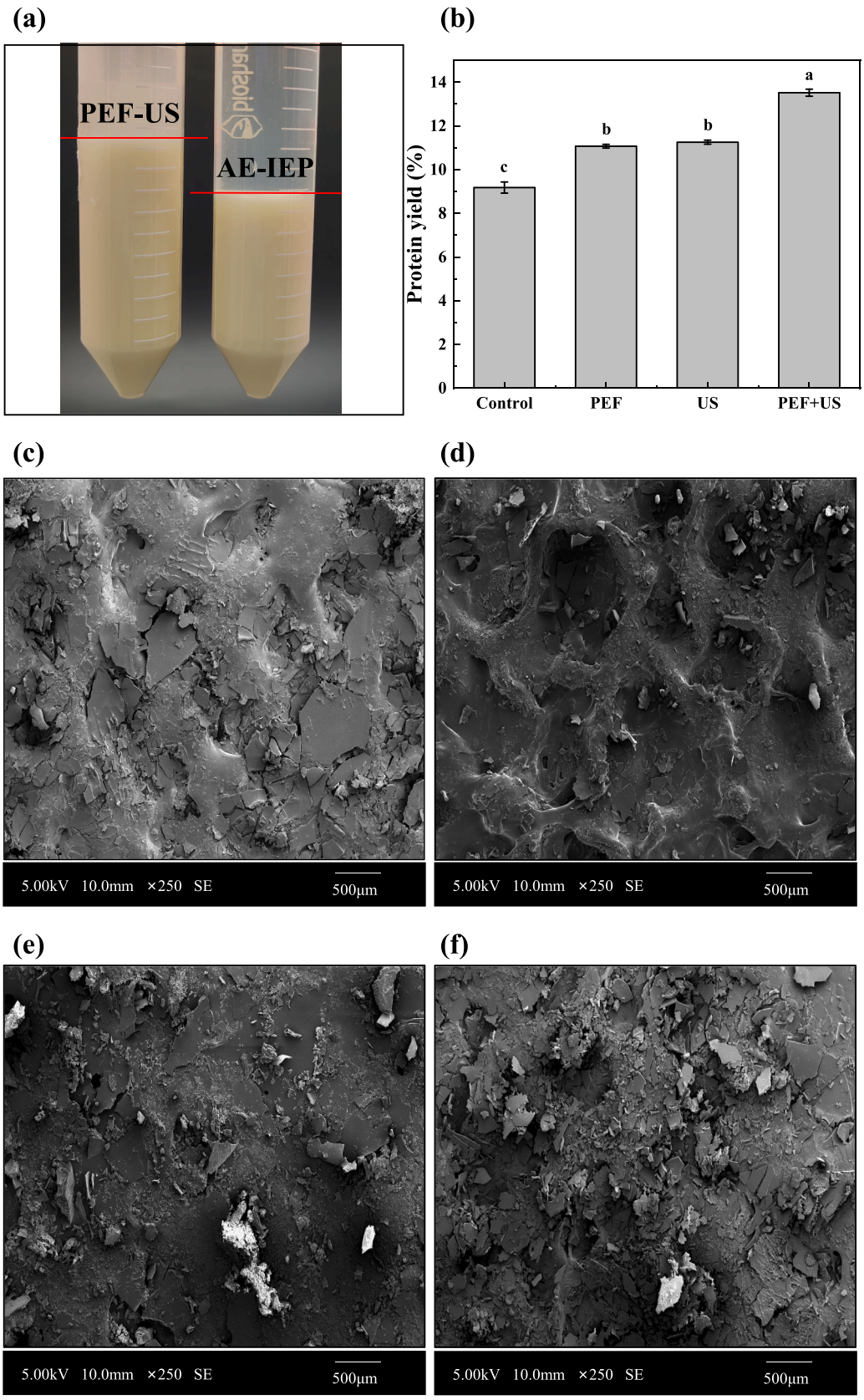

Fig. 4. (a) Experimental pictures of isoelectric point precipitation by PEF-US and AE-IEP treatment, (b) Effect of four different treatments on CPI yield, (c)-(f) Surface topography of CPI obtained from AE-IEP, PEF, US and PEF-US treatment, respectively.

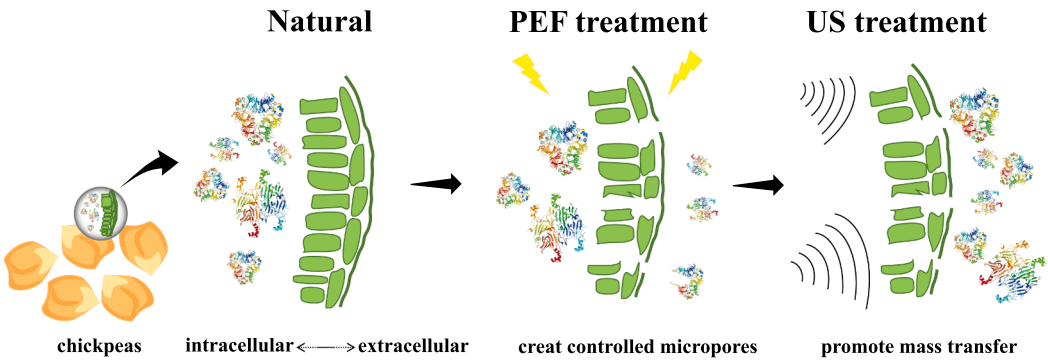

Fig. 5. Mechanism of CPI extraction by PEF-US: PEF treatment first induces electroporation to form controlled micropores, followed by US treatment to promote mass transfer.

3.6. Surface morphology observation

The morphology of CPI obtained from AE-IEP, PEF, US and PEF-US treatment were shown in Fig. 4c-f. After AE-IEP treatment, the protein surface exhibited a smooth and dense block structure with significant block aggregation (Fig. 4c). In Fig. 4d, the protein surface displayed a distinct pitted morphology after PEF treatment. The appearance of the craters is likely to be related to the localized loosening and subsequent collapse of the proteins due to the electric field stress under PEF partial discharge [33]. The protein surface treated with US, as shown in Fig. 4e, appeared looser and more fragmented in overall morphology. This phenomenon resulted from the cavitation effect generated by the ultrasonic treatment, which produced mechanical shear force that ruptured the intact protein lamellae and turned them into fragments [34]. Furthermore, the degree of fragmentation was notably higher in both the PEF and US groups compared to the AE-IEP group, which may be more favorable for CPI dissolution. After the combined PEF-US treatment, the protein surface represented a loose fragmented structure with significantly improved aggregation, and the degree of fragmentation was the highest among all treatment groups. This was possible because, with the PEF-US treatment, the US had further dispersed the protein, building upon the PEF treatment, which resulted in more protein fragments and a looser structure.

3.7. Influence on secondary structure content

The effect of PEF and US treatment on the secondary structure of CPI was analyzed by CD spectroscopy. The changes in the secondary structure content of native and treated CPI were measured in the near-ultraviolet spectra from 200 nm to 260 nm. Table 3 exhibited that the α-helix, β-sheet, β-turn, and random coil of natural CPI were 27.55 %, 19.92 %, 17.39 %, and 35.14 %, respectively. The β-turn content of CPI after PEF treatment increased significantly ($P < 0.05$), the α-helix content decreased slightly, and the β-sheet and random coil increased slightly. This was similar to conclusion described by Wang et al. [35]. It was probably the PEF treatment caused the disulfide bonds in the secondary structure of CPI to break and hydrogen bonds to be disrupted, which resulted in the conversion of some of the α-helix into β-sheet, β-turn with random coil. Some studies had shown that a decrease in protein α-helix content and an increase in β-sheet content was favorable to improve the functional properties of proteins [36]. The US-treated CPI exhibited a slight increase in α-helix content, a significant decrease in β-sheet and β-turn content ($P < 0.05$), and a slight decrease in random coil content. This was similar to conclusion reported by Vera et al. [37]. But Zhu et al. [38] found that US treatment decreased the α-helix content and increased the β-sheet content of the protein, which might be the conditions of the US treatment as well as differences in the type of protein. Addition of US-treated CPI under PEF treatment resulted in significant changes in the content of all four structures compared with natural CPI, with a significant decrease in α-helix content ($P < 0.05$) and a significant increase in the content of β-sheet, β-turn, and random coil ($P < 0.05$). The PEF-US treatment led to a further α-helix to β-sheet, β-turn, and random coil in CPI transformation. This indicated that the combined treatment resulted in a more pronounced change in the secondary structure of CPI, from the originally stable α-helix structure to a more loosely packed random coil state.

Table 3
Secondary structure content of native and treated CPI.

Treatment	Content of each structure/Total structural contenteld (%)			
	α-helix	β-sheet	β-turn	Random coil
AE-IEP	27.55 ± 0.84^{ab}	19.92 ± 0.34^{b}	17.39 ± 0.02^{b}	35.14 ± 0.41^{b}
PEF	26.76 ± 0.17^{b}	20.31 ± 0.08^{b}	17.49 ± 0.02^{a}	35.47 ± 0.06^{b}
US	28.52 ± 0.57^{a}	19.32 ± 0.25^{c}	17.12 ± 0.06^{c}	35.01 ± 0.29^{b}
PEF-US	17.77 ± 0.07^{c}	24.95 ± 0.03^{a}	17.56 ± 0.03^{a}	39.72 ± 0.01^{a}

3.8. Influence on tertiary structure content

Intrinsic fluorescence spectroscopy can reflect the changes in the microenvironment of aromatic amino acids [39]. When the emission wavelength was 280 nm, it can expose the tryptophan, tyrosine and phenylalanine residues of protein to the surface of the molecule. Therefore, the variations in the tertiary structure of proteins can be directly characterized by the changes in the intensity of fluorescence and the position of the peak [40]. Fig. 6a showed that the wavelength of the maximum fluorescence peak of AE-IEP CPI was at 323 nm, while the maximum fluorescence peak of PEF, US, and PEF-US CPI were red-shifted. Among them, the PEF-US group showed the largest red-shift from 323 nm to 325 nm. The fluorescence intensities of CPI were all increased after treatment with different extraction methods, which indicated that the tertiary structure of CPI unfolded, and the side-chain groups of the aromatic amino acid molecules inside CPI were exposed and migrated to a more hydrophilic environment. In conclusion, PEF, US and PEF-US treatment all altered the tertiary structure of CPI, with PEF-US having the greatest effect on the tertiary structure of CPI.

3.9. Influence on surface hydrophobicity

In general, changes in the structure of a protein could be reflected by its surface hydrophobicity. It also exerted a vitally significant effect on the functional properties of the protein [41]. As can be seen from Fig. 6b, the surface hydrophobicity of treated CPI was remarkably increased ($p < 0.05$) compared with natural CPI. The PEF, US and PEF-US CPI showed an increase of 23.36 %, 19.60 % and 52.97 % respectively compared to the AE-IEP CPI. This was similar to the conclusion of Wang et al., reported [42]. This phenomenon was attributed to the unfolding of protein molecules and loosening of the protein structure by PEF

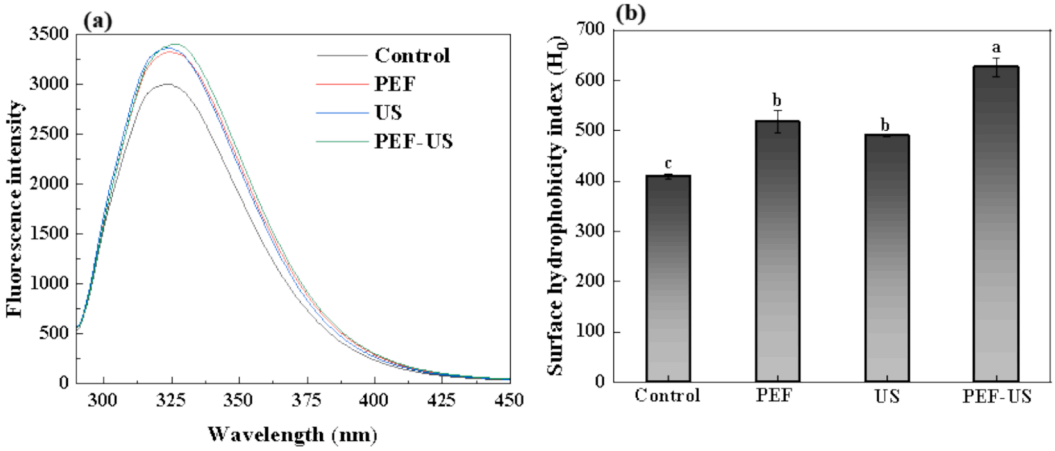

Fig. 6. (a) Fluorescence spectra and (b) surface hydrophobicity of CPI after different treatments. Different letters denote significant differences in the components ($p < 0.05$).

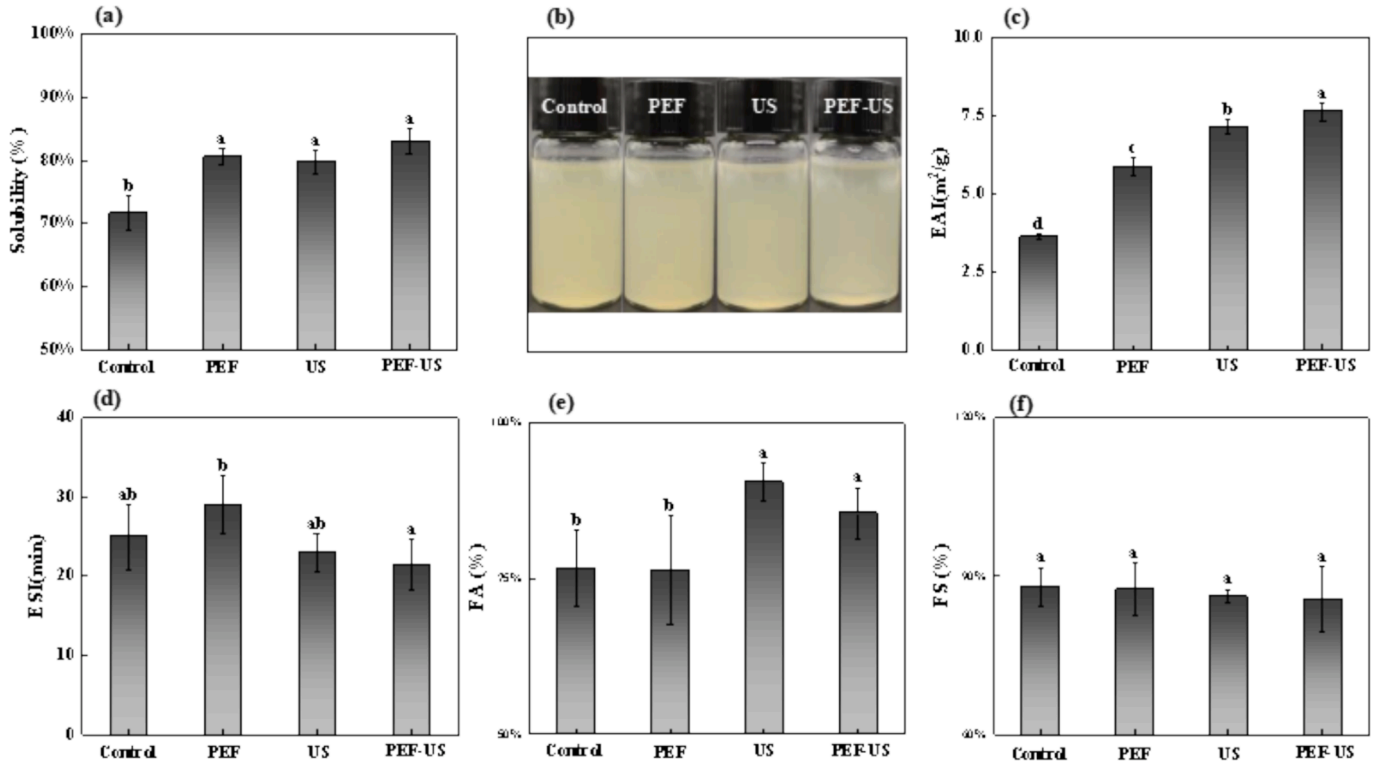

Fig. 7. (a) Solubility, (b) Appearance of samples after dissolution, (c) Emulsification, (d) Emulsion stability, (e) Foaming and (f) Foaming stability of CPI after different treatment.

treatment, thus allowing ANS molecules to reach the hydrophobic core of the protein disrupting the hydrophobic interactions between protein molecules and increased the exposure of hydrophobic groups [43]. Meanwhile, the cavitation effect generated by the US treatment could lead to further unfolding of protein molecules, protein molecule extension and more exposure of hydrophobic groups, which in turn improved the surface hydrophobicity of CPI [44].

3.10. Influence on solubility of CPI

Solubility was considered to be the most important practical indicator of the functional properties of protein, and it was an important functional property to satisfy the protein to exert their emulsification, foaming and gelation properties. Fig. 7a, b showed that the solubility of CPI was significantly increased by different modification treatments ($p < 0.05$), and the PEF, US and PEF-US CPI increased by 8.85 %, 8.03 % and 11.31 %, respectively, compared with AE-IEP CPI. The best solubility enhancement after the combined treatment was mainly due to the fact that the PEF treatment firstly broke the non-covalent bonds between protein molecules, which led to the unfolding of their structures from the compact state, and then transformed the aggregated protein molecules into independent single molecules. This process significantly enhanced the interaction force between the protein molecules and the solvent, thus improving the solubility of the proteins [43,45]. Next, the US treatment further unfolded the structure of protein molecules by disrupting intermolecular strong interactions through cavitation effect, including Van der Waals forces, hydrogen bonding and dipole attractions, exposing more hydrophilic regions, which further enhanced the

interaction with the solute [46], thus improving the solubility.

3.11. Influence on emulsification properties of CPI

The emulsifying properties of protein, namely, its ability to form and stabilize emulsions, played an important role in the food manufacturing industry [47]. Fig. 7c exhibited a significant ($p < 0.05$) increase in emulsifing capacity (EAI) of CPI treated with different conditions of modification. The CPI of PEF, US, and PEF-US treatment were increased by 61.31 %, 96.08 %, and 109.61 %, respectively, compared to natural CPI. This was due to the fact that PEF treatment polarized and partially unfolded the protein molecules, and meanwhile exposed the hydrophobic residues inside the proteins, which increased the surface hydrophobicity and lowered the interfacial tension [48]. At the same time, the cavitation effect of US treatment caused the protein molecules to unfold, exposing the hydrophobic groups embedded in the molecules, resulting in a further increase in the surface hydrophobicity, promoting the rapid absorption of proteins at the oil–water interface, and the interfacial tension was further reduced to further enhance the emulsification ability [49]. Nevertheless this was corroborated by the fact that there was no significant change in any of the data sets in Fig. 7d. The emulsification properties of proteins might be related to the size of the droplets [38], but with the extension of time, intermolecular aggregation would occur, which might lead to an increase in droplet size and a decrease in surface activity, making it difficult to enhance the stability of emulsification.

3.12. Influence on foaming properties of CPI

Foam is another important functional property of proteins, and the fine foam once formed by CPI can provide good flavor to foods. After calculating the foaming ability (FA) by the formula, it could be seen from Fig. 7e that the FA values of PEF-US treated and US treated were significantly ($p < 0.05$) increased, by 12.02 % and 17.93 %, respectively, compared to the native CPI. The increased FA values of the US treated and PEF-US treated CPI were attributed to its higher surface hydrophobicity and more flexible structure (higher random coil content), which resulted in an enhanced ability of the protein to form liquid–air dispersions and a lower interfacial tension, favoring the formation of gas bubbles [50]. However, the foam stability (FS) of CPI treated with different modification conditions was not improved, and the bubbles dispersed in large quantities after 30 min, and there was no significant difference in their FS as shown in Fig. 7f. This was probably due to the fact that after a certain period of time, the size of the bubbles increased and the molecules were desorbed at the interface, leading to an increase in the exposure of hydrophobic groups, which made the proteins easily aggregated and reduced the protein interfacial activity, resulting in the formation of FS similar to that of the untreated group [50].

4. Conclusion

PEF-US is an effective method to extract CPI. The extraction parameters were optimized using RSM, resulting in the following conditions: 87 s pulse duration, 0.9 kV/cm electric field intensity, 15 min ultrasonic time, and 325 W ultrasonic power. Under these optimized conditions, the protein yield was measured at 13.52 ± 0.13 %, which was a 47.28 % improvement compared to the AE-IEP treatment. In addition, PEF-US treatment also exhibited higher yield compared to the PEF and US treatment. The surface of PEF-US-treated CPI was looser, with less protein aggregation, and the structure of CPI showed greater extensibility and disorder in characterizing secondary and tertiary structures. The modified CPI shows improved water solubility, emulsification, and foaming capabilities, indicating enhanced potential as an emulsifier and foaming agent in the food industry. Overall, the utilization of PEF-US treatment proved to be effective in increasing protein yield and enhancing its functional properties, thereby adding value to chickpea in the realm of food processing.

CRediT authorship contribution statement

Xin-Jue Lai: Writing – original draft, Software, Methodology, Formal analysis, Data curation. **Jian-Quan Chen:** Writing – original draft, Software, Methodology, Formal analysis, Data curation. **Jing Nie:** Writing – review & editing. **Pei-Feng Guo:** Writing – review & editing. **Muhammad Faisal Manzoor:** Writing – review & editing, Methodology. **Yan-Yan Huang:** Writing – review & editing, Methodology. **Jian Li:** Writing – review & editing, Software, Methodology, Funding acquisition. **Song-Yi Lin:** Writing – review & editing, Software, Methodology. **Xin-An Zeng:** Writing – review & editing, Software, Methodology, Funding acquisition. **Rui Wang:** Writing – review & editing, Software, Methodology, Formal analysis, Data curation, Conceptualization.

Declaration of competing interest

The authors declare that they have no known competing financial interests or personal relationships that could have appeared to influence the work reported in this paper.

Acknowledgements

The authors are grateful to the National Natural Science Foundation of China (Grant no. U23A20267, 32172348 & 31972205), National Key Research and Development Program of China (Grant 2023YFD2101000), Guangdong Provincial Department of Agriculture and Rural Affairs Agricultural Research and Technology Promotion Demonstration (Grant No. 2023KJ144), Key Laboratory Project of Guangdong Province (Grant No. 2022B1212010015), the China Postdoctoral Science Foundation (2022M721196) and the Guangdong Basic and Applied Basic Research Foundation (2022A1515110186).

Appendix A. Supplementary data

Supplementary data to this article can be found online at https://doi.org/10.1016/j.ultsonch.2024.107089.

References

[1] J. Huang, L.M. Liao, S.J. Weinstein, R. Sinha, B.I. Graubard, D. Albanes, Association between plant and animal protein intake and overall and cause-specific mortality, JAMA Intern. Med. 180 (2020) 1173–1184, https://doi.org/10.1001/jamainternmed.2020.2790.
[2] K.S. Poutanen, A.O. Kårlund, C. Gómez-Gallego, D.P. Johansson, N.M. Scheers, I. M. Marklinder, A.K. Eriksen, P.C. Silventoinen, E. Nordlund, N. Sozer, K. J. Hanhineva, M. Kolehmainen, R. Landberg, Grains – a major source of sustainable protein for health, Nutr. Rev. 80 (2022) 1648–1663, https://doi.org/10.1093/nutrit/nuab084.
[3] M. Vogelsang-O'Dwyer, E. Zannini, E.K. Arendt, Production of pulse protein ingredients and their application in plant-based milk alternatives, Trends Food Sci. Technol. 110 (2021) 364–374, https://doi.org/10.1016/j.tifs.2021.01.090.
[4] L.H. Fasolin, R.N. Pereira, A.C. Pinheiro, J.T. Martins, C.C.P. Andrade, O.L. Ramos, A.A. Vicente, Emergent food proteins – Towards sustainability, health and innovation, Food Res. Int. 125 (2019) 108586, https://doi.org/10.1016/j.foodres.2019.108586.
[5] P.J. Strong, R. Self, K. Allikian, E. Szewczyk, R. Speight, I. O'Hara, M.D. Harrison, Filamentous fungi for future functional food and feed, Curr. Opin. Biotechnol. 76 (2022) 102729, https://doi.org/10.1016/j.copbio.2022.102729.
[6] S. Bleakley, M. Hayes, Algal proteins: extraction, application, and challenges concerning production, Foods 6 (2017) 33, https://doi.org/10.3390/foods6050033.
[7] D.E. Garcia-Valle, L.A. Bello-Pérez, E. Agama-Acevedo, J. Alvarez-Ramirez, Structural characteristics and in vitro starch digestibility of pasta made with durum wheat semolina and chickpea flour, LWT 145 (2021) 111347, https://doi.org/10.1016/j.lwt.2021.111347.
[8] N. Grasso, N.L. Lynch, E.K. Arendt, J.A. O'Mahony, Chickpea protein ingredients: A review of composition, functionality, and applications, Compr. Rev. Food Sci. Food Saf. 21 (2022) 435–452, https://doi.org/10.1111/1541-4337.12878.

[9] B.P. Yaputri, S. Feyzi, B.P. Ismail, Transglutaminase-induced polymerization of pea and chickpea protein to enhance functionality, Gels 10 (2023) 11, https://doi.org/10.3390/gels10010011.
[10] A.C.Y. Lam, K.C. Karaca, R.T. Tyler, M.T. Nickerson, Pea protein isolates: Structure, extraction, and functionality, Food Rev. Int. 34 (2016) 126–147, https://doi.org/10.1080/87559129.2016.1242135.
[11] Z. Gao, P. Shen, Y. Lan, L. Cui, J.B. Ohm, B. Chen, J. Rao, Effect of alkaline extraction pH on structure properties, solubility, and beany flavor of yellow pea protein isolate, Food Res. Int. 131 (2020) 109045, https://doi.org/10.1016/j.foodres.2020.109045.
[12] C.H. Edwards, P. Ryden, G. Mandalari, P.J. Butterworth, P.R. Ellis, Structure–function studies of chickpea and durum wheat uncover mechanisms by which cell wall properties influence starch bioaccessibility, Nat. Food 2 (2021) 118–126, https://doi.org/10.1038/s43016-021-00230-y.
[13] Y. Ma, J. Zhang, J. He, Y. Xu, X. Guo, Effects of high-pressure homogenization on the physicochemical, foaming, and emulsifying properties of chickpea protein, Food Res. Int. 170 (2023) 112986, https://doi.org/10.1016/j.foodres.2023.112986.
[14] N.L. Ruiz-Zambrano, E. Pérez-Carrillo, S.O. Serna-Saldívar, V. Tejada-Ortigoza, Effect of thermal, nonthermal, and combined treatments on functional and nutritional properties of chickpeas, Crit. Rev. Food Sci. Nutr. (2023) 1–19, https://doi.org/10.1080/10408398.2023.2237577.
[15] M. Kumar, M. Tomar, J. Potkule, R. Verma, S. Punia, A. Mahapatra, T. Belwal, A. Dahuja, S. Joshi, M.K. Berwal, V. Satankar, A.G. Bhoite, R. Amarowicz, C. Kaur, J.F. Kennedy, Advances in the plant protein extraction: Mechanism and recommendations, Food Hydrocolloids 115 (2021) 106595, https://doi.org/10.1016/j.foodhyd.2021.106595.
[16] M. Kronbauer, I. Shorstkii, S.B. da Silva, S. Toepfl, A. Lammerskitten, C. Siemer, Pulsed electric field assisted extraction of soluble proteins fromnettle leaves (Urtica dioica L.): kinetics and optimization using temperature and specific energy. Sustainable, Food Technol. 1 (2023) 886–895, https://doi.org/10.1039/D3FB00053B.
[17] M.J. Tan, Y. Li, S.Q. Zhao, F.H. Yue, D.J. Cai, J.T. Wu, X.A. Zeng, J. Li, Z. Han, Synergistic ultrasound pulsed electric field extraction of litchi peel polyphenols and determination of their properties, Int. J. Biol. Macromol. 260 (2024) 129613, https://doi.org/10.1016/j.ijbiomac.2024.129613.
[18] J. Zhan, Z. Liang, J. Li, X.A. Zeng, G. Ou, C. Zhong, Pulsed electric field-ultrasonic assisted extraction combined with macroporous resin for the preparation of flavonoids from Pericarpium Citri Reticulatae, J. Food Process. Preserv. 46 (2022) e16823.
[19] B. Byanju, M.M. Rahman, M.P.H. Evangelista, B.P. Lamsal, Effect of high-power sonication pretreatment on extraction and some physicochemical properties of proteins from chickpea, kidney bean, and soybean, Int. J. Biol. Macromol. 145 (2020) 712–721, https://doi.org/10.1016/j.ijbiomac.2019.12.118.
[20] L. Chang, Y. Lan, N. Bandillo, J.B. Ohm, B. Chen, J. Rao, Plant proteins from green pea and chickpea: Extraction, fractionation, structural characterization and functional properties, Food Hydrocolloids 123 (2022) 107165, https://doi.org/10.1016/j.foodhyd.2021.107165.
[21] M. Mousazadeh, M. Mousavi, G. Askari, H. Kiani, I. Adt, A. Gharsallaoui, Thermodynamic and physiochemical insights into chickpea protein-Persian gum interactions and environmental effects, Int. J. Biol. Macromol. 119 (2018) 1052–1058, https://doi.org/10.1016/j.ijbiomac.2018.07.168.
[22] G.W. Latimer (Ed.), Official Methods of Analysis of AOAC International (20th ed.), Rockville, MA (2016).
[23] W. Xiong, Y. Wang, C. Zhang, J. Wan, B.R. Shah, Y. Pei, B. Zhou, J. Li, B. Li, High intensity ultrasound modified ovalbumin: structure, interface and gelation properties, Ultrason. Sonochem. 31 (2016) 302–309, https://doi.org/10.1016/j.ultsonch.2016.01.014.
[24] R. Wang, M.Q. Zeng, Y.W. Wu, Y.X. Teng, L.H. Wang, J. Li, F.Y. Xu, B.R. Chen, Z. Han, X.A. Zeng, Enhanced encapsulation of lutein using soy protein isolate nanoparticles prepared by pulsed electric field and pH shifting treatment, Food Chem. 424 (2023) 136386, https://doi.org/10.1016/j.foodchem.2023.136386.
[25] N.D. Patil, A. Bains, S. Kaur, R. Yadav, N. Ali, S. Patil, G. Goksen, P. Chawla, Influence of dual succinylation and ultrasonication modification on the amino acid content, structural and functional properties of Chickpea (Cicer arietinum L.) protein concentrate, Food Chem. 445 (2024) 138671, https://doi.org/10.1016/j.foodchem.2024.138671.
[26] M. Tan, J. Xu, H. Gao, Z. Yu, J. Liang, D. Mu, X. Li, X. Zhong, S. Luo, Y. Zhao, S. Jiang, Z. Zheng, Effects of combined high hydrostatic pressure and pH-shifting pretreatment on the structure and emulsifying properties of soy protein isolates, J. Food Eng. 306 (2021) 110622, https://doi.org/10.1016/j.jfoodeng.2021.110622.
[27] Y. Zhang, M. Ishikawa, S. Koshio, S. Yokoyama, S. Dossou, W. Wang, X. Zhang, R. S. Shadrack, K. Mzengeraze, K. Zhu, S. Seo, Optimization of soybean meal fermentation for aqua-feed with Bacillus subtilis natto using the response surface methodology, Fermentation 7 (2021) 306, https://doi.org/10.3390/fermentation7040306.
[28] A. Kamboj, R. Chopra, R. Singh, V. Saxena, P.K. Gv, Effect of pulsed electric field parameters on the alkaline extraction of valuable compounds from perilla seed meal and optimization by central composite design approach, Appl. Food Res. 2 (2022) 100240, https://doi.org/10.1016/j.afres.2022.100240.
[29] R.S. Das, B.K. Tiwari, F. Chemat, M. Garcia-Vaquero, Impact of ultrasound processing on alternative protein systems: protein extraction, nutritional effects and associated challenges, Ultrason. Sonochem. 91 (2022) 106234, https://doi.org/10.1016/j.ultsonch.2022.106234.
[30] R. Vardanega, D.T. Santos, M.A.A. Meireles, Intensification of bioactive compounds extraction from medicinal plants using ultrasonic irradiation, Pharmacogn. Rev. 8 (2014) 88–95, https://doi.org/10.4103%2F0973-7847.134231.
[31] R. Bocker, E.K. Silva, Pulsed electric field assisted extraction of natural food pigments and colorings from plant matrices, Food Chem.: X 15 (2022) 100398, https://doi.org/10.1016/j.fochx.2022.100398.
[32] Y. Qi, F. Yu, X. Wang, N. Wan, M. Yang, Z. Wu, Y. Li, Drying of wolfberry fruit juice using low-intensity pulsed ultrasound, Lwt 141 (2021) 110953, https://doi.org/10.1016/j.lwt.2021.110953.
[33] T. Grgić, R. Bleha, P. Smrčkova, V. Stulić, T.V. Pavičić, A. Synytsya, D. Lveković, D. Novotni, Pulsed electric field treatment of oat and barley flour: influence on enzymes, non-starch polysaccharides, dough rheological properties, and application in flat bread, Food Bioprocess Technol. (2024) 1–22, https://doi.org/10.1007/s11947-024-03383-3.
[34] J. Xu, S. Yan, J. Xu, B. Qi, Ultrasound-assisted modification of soybean protein isolate with L-histidine: Relationship between structure and function, Ultrason. Sonochem. 107 (2024) 106934, https://doi.org/10.1016/j.ultsonch.2024.106934.
[35] R. Wang, Q.H. Wen, X.A. Zeng, J.W. Lin, J. Li, F.Y. Xu, Binding affinity of curcumin to bovine serum albumin enhanced by pulsed electric field pretreatment, Food Chem. 377 (2022) 131945, https://doi.org/10.1016/j.foodchem.2021.131945.
[36] R.M. Rodrigues, Z. Avelar, A.A. Vicente, S.B. Petersen, R.N. Pereira, Influence of moderate electric fields in β-lactoglobulin thermal unfolding and interactions, Food Chem. 304 (2020) 125442, https://doi.org/10.1016/j.foodchem.2019.125442.
[37] A. Vera, M.A. Valenzuela, M. Yazdani-Pedram, C. Tapia, L. Abugoch, Conformational and physicochemical properties of quinoa proteins affected by different conditions of high-intensity ultrasound treatments, Ultrason. Sonochem. 51 (2018) 186–196, https://doi.org/10.1016/j.ultsonch.2018.10.026.
[38] Z. Zhu, W. Zhu, J. Yi, N. Liu, Y. Cao, J. Lu, E.A. Decker, D.J. McClements, Effects of sonication on the physicochemical and functional properties of walnut protein isolate, Food Res. Int. 106 (2018) 853–861, https://doi.org/10.1016/j.foodres.2018.01.060.
[39] Z. Zhu, X. Mao, Q. Wu, J. Zhang, X. Deng, Effects of oxidative modification of peroxyl radicals on the structure and foamability of chickpea protein isolates, J. Food Sci. 86 (2021) 824–833, https://doi.org/10.1111/1750-3841.15643.
[40] S. Kang, J. Zhang, X. Guo, Y. Lei, M. Yang, Effects of ultrasonic treatment on the structure, functional properties of chickpea protein isolate and its digestibility in vitro, Foods 11 (2022) 880, https://doi.org/10.3390/foods11060880.
[41] L. Chen, J. Chen, J. Ren, M. Zhao, Effects of ultrasound pretreatment on the enzymatic hydrolysis of soy protein isolates and on the emulsifying properties of hydrolysates, Agric. Food Chem. 59 (2011) 2600–2609, https://doi.org/10.1021/jf103771x.
[42] R. Wang, L.H. Wang, Q.H. Wen, F. He, F.Y. Xu, B.R. Chen, X.A. Zeng, Combination of pulsed electric field and pH shifting improves the solubility, emulsifying, foaming of commercial soy protein isolate, Food Hydrocolloids 134 (2023) 108049, https://doi.org/10.1016/j.foodhyd.2022.108049.
[43] B.Y. Xiang, M.O. Ngadi, L.A. Ochoa-Martinez, M.V. Simpson, Pulsed electric field-induced structural modification of whey protein isolate, Food Bioprocess Technol. 4 (2011) 1341–1348, https://doi.org/10.1007/s11947-009-0266-z.
[44] H. Cao, R. Sun, J. Shi, M. Li, X. Guan, J. Liu, K. Huang, Y. Zhang, Effect of ultrasonic on the structure and quality characteristics of quinoa protein oxidation aggregates, Ultrason. Sonochem. 77 (2021) 105685, https://doi.org/10.1016/j.ultsonch.2021.105685.
[45] X. Hu, H. Wang, Y. Hu, Z. Tu, Insight into the effects of pulsed electric field on the structure, aggregation characteristics and functional properties of whey proteins, Food Hydrocolloids 154 (2024) 110111, https://doi.org/10.1016/j.foodhyd.2024.110111.
[46] Y. Li, Y. Cheng, Z. Zhang, Y. Wang, B.K. Mintah, M. Dabbour, H. Jiang, R. He, H. Ma, Modification of rapeseed protein by ultrasound-assisted pH shift treatment: Ultrasonic mode and frequency screening, changes in protein solubility and structural characteristics, Ultrason. Sonochem. 69 (2020) 105240, https://doi.org/10.1016/j.ultsonch.2020.105240.
[47] Y. Meng, Z. Liang, C. Zhang, S. Hao, H. Han, P. Du, A. Li, H. Shao, C. Li, L. Liu, Ultrasonic modification of whey protein isolate: Implications for the structural and functional properties, LWT 152 (2021) 112272, https://doi.org/10.1016/j.lwt.2021.112272.
[48] A. Taha, F. Casanova, P. Šimonis, V. Stankevič, M.A.E. Gomaa, A. Stirkė, Pulsed electric field: fundamentals and effects on the structural and techno-functional properties of dairy and plant protein, Foods 11 (2022) 1556, https://doi.org/10.3390/foods11111556.
[49] Q. Zhao, T. Xie, X. Hong, Y. Zhou, L. Fan, Y. Liu, J. Li, Modification of functional properties of perilla protein isolate by high-intensity ultrasonic treatment and the stability of o/w emulsion, Food Chem. 368 (2022) 130848, https://doi.org/10.1016/j.foodchem.2021.130848.
[50] Y. Wang, S. Wang, R. Li, Y. Wang, Q. Xiang, K. Li, Y. Bai, Effects of combined treatment with ultrasound and pH shifting on foaming properties of chickpea protein isolate, Food Hydrocolloids 124 (2022) 107351, https://doi.org/10.1016/j.foodhyd.2021.107351.